Enhanced Simple Linear Iterative Clustering (ESLIC) for Precise Skin Lesion Segmentation in Dermoscopic Images

Leni Natalia Zulita[1]*, Sarjon Defit[2], Sumijan[3]
Information Engineering, Faculty of Computer Science, Dehasen University, Bengkulu, Indonesia[1]
Faculty of Computer Science, University of Putra Indonesia YPTK, Padang, Indonesia[2, 3]

***Abstract*—The main challenge in dermoscopy image analysis lies in the lesion segmentation process, which is often affected by variations in color, texture, lighting, and irregular lesion boundaries. The Simple Linear Iterative Clustering (SLIC) method is widely used for superpixel-based segmentation, but it still faces limitations in preserving the morphological details of lesions in complex areas. This study proposes Enhanced Simple Linear Iterative Clustering (ESLIC) as a new approach to improve the quality of skin lesion segmentation. ESLIC combines a dynamic compactness adjustment mechanism, local texture analysis, and gradient-based boundary refinement to generate superpixels that are more adaptive to image characteristics. The study was conducted using 277 dermoscopy images consisting of benign lesions and melanoma lesions. Before segmentation, the images underwent image enhancement through filtering, normalization, contrast enhancement, and sharpening. ESLIC's performance was evaluated based on segmentation quality and its impact on the classification process using a Convolutional Neural Network (CNN). The experimental results show that ESLIC is capable of producing a more accurate representation of lesion areas compared to conventional superpixel methods, particularly in areas with heterogeneous textures and complex lesion boundaries. The findings of this study indicate that ESLIC can improve the effectiveness of feature extraction and has the potential to become a key component in the development of artificial intelligence-based melanoma diagnosis support systems.**

***Keywords*—ESLIC; dermoscopy; melanoma; SLIC; superpixel; CNN**

I. Introduction

Advances in digital image processing and artificial intelligence have made significant contributions across various fields, particularly in the healthcare sector. The use of digital images enables medical analysis to be conducted more objectively, quickly, and accurately than with conventional visual examinations. One application that is currently growing rapidly is the use of computer-aided diagnosis (CAD) systems to assist medical professionals in the early detection of various diseases. These systems utilize image processing techniques, machine learning, and deep learning to extract important information from medical images, thereby supporting the clinical decision-making process more effectively [1], [2].

One disease of global concern is melanoma, a type of skin cancer that originates in melanocytes and has a high mortality rate if not detected in its early stages. Melanoma is known as one of the most aggressive forms of skin cancer because it metastasizes rapidly to other tissues in the body. Therefore, early detection is a critical factor in improving treatment success rates and prolonging patients' life expectancy [3].

In clinical practice, one of the technologies widely used to aid in the diagnosis of melanoma is dermoscopy [4], [5]. Dermoscopy is a non-invasive imaging technique that allows doctors to observe the morphological structure of the skin in greater detail than a standard visual examination. Through dermoscopy images, lesion characteristics such as color variations, pigment patterns, border shapes, and blood vessel distribution can be observed more clearly [6]. However, the interpretation of dermoscopy images still relies heavily on the clinical experience of dermatologists, which can lead to diagnostic variability among observers. Therefore, an artificial intelligence-based automated diagnostic system offers a promising solution for improving the consistency and objectivity of diagnoses [7].

One of the most important steps in a dermoscopy image analysis system is image segmentation. Segmentation aims to separate the lesion area from normal skin tissue so that feature extraction and classification can focus on the relevant areas. Various studies have shown that segmentation quality has a direct impact on improving the accuracy of AI-based skin lesion classification. Accurate segmentation allows classification models to learn the morphological characteristics of lesions more effectively, thereby improving the performance of automated diagnostic systems [8], [9].

Nevertheless, skin lesion segmentation remains a complex challenge. Variations in skin color, uneven lighting, presence of hair, light reflections, heterogeneous lesion textures, and irregular lesion boundaries often lead to segmentation errors. These complexities cause conventional segmentation methods to frequently produce imprecise object boundaries, thereby reducing the overall performance of the diagnostic system [10].

Among the various segmentation approaches that have been developed, superpixel-based methods are among the most widely used techniques because they can group pixels with similar characteristics into homogeneous regions.

*Corresponding author

One of the most popular superpixel algorithms is Simple Linear Iterative Clustering (SLIC) [11]. This algorithm offers high computational efficiency and the ability to generate superpixels with good spatial structure. However, SLIC still has limitations when applied to dermoscopy images because it relies solely on color and spatial information during the pixel clustering process. As a result, segmentation often fails to follow complex lesion boundaries, particularly in areas with heterogeneous textures and low contrast [12], [13].

Several studies have sought to improve the quality of skin lesion segmentation by integrating texture features, gradients, or deep learning-based approaches [14]. However, most studies still focus on improving segmentation quality in general and have not specifically developed a superpixel mechanism that adapts to changes in local image characteristics. Furthermore, preserving lesion boundaries remains a challenge that needs to be addressed to produce more accurate and consistent segmentation under various dermoscopy image conditions [15], [16].

Based on these issues, this study proposes the Enhanced Simple Linear Iterative Clustering (ESLIC) method as an extension of the SLIC algorithm to improve the quality of skin lesion segmentation in dermoscopy images. ESLIC is designed by integrating mechanisms for adaptive compactness adjustment, texture-aware clustering, gradient-aware feature integration, and boundary refinement. Unlike conventional SLIC, which uses a fixed compactness parameter, ESLIC adaptively adjusts this parameter based on local texture characteristics, thereby generating superpixels that are more representative of the lesion's structure. Furthermore, the integration of texture and gradient information is expected to improve the algorithm's ability to preserve lesion boundaries more accurately.

This study used dermoscopy images obtained from Dr. M. Djamil General Hospital in Padang as the research subjects. The ESLIC segmentation results were then used as input for a Convolutional Neural Network (CNN) model to evaluate the effect of segmentation quality on the performance of skin lesion classification. Thus, this study is expected to provide a theoretical contribution to the development of superpixel-based segmentation methods and a practical contribution to supporting a more accurate, faster, and more reliable melanoma early detection system.

Moreover, For CNNs, the detailed description begins with the architecture or layer configuration, which consists of the number of layers, filter size, pooling type, output layer, and other parameters. in addition, there are activation functions, namely the activation in the hidden layer (ReLU) and the activation in the output layer (Sigmoid for binary classification or softmax), as well as the training protocol, which consists of the number of epochs, batch size, optimizer, dataset (e.g., 277 images for the training and validation processes), and additional hyperparameters. Fig. 1 illustrates the CNN architecture used in this study.

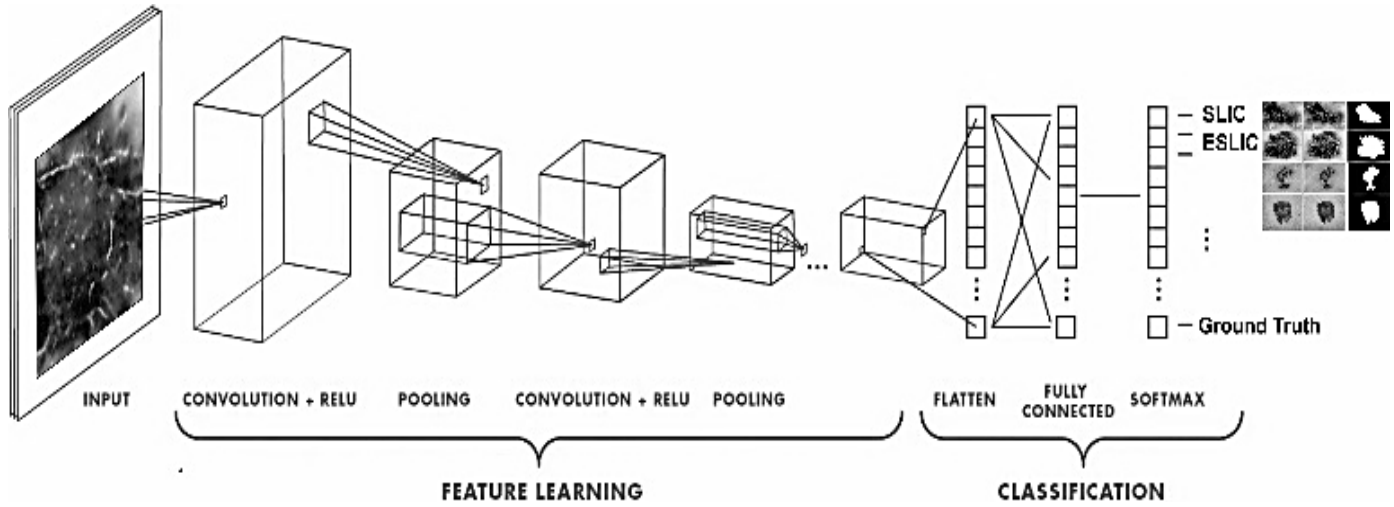

Fig. 1. Convolutional Neural Network (CNN) architecture

II. Related Work

There are key references indicating that previous research has been conducted by researchers on topics such as Superpixel-Oriented Label Distribution Learning [13], a hierarchical three-step superpixels and deep learning framework for skin lesion classification [31], transfer learning and hybrid feature extraction for medical segmentation [9], SAM -Adapters plus Vision Transformers for skin lesion segmentation [29], and SPADE, a superpixel adjacency method for 3-class melanoma segmentation. Specific details can be found in Table I.

TABLE I. RELATED WORK FROM PREVIOUS RESEARCH AND RELATED METHODS

Research Topics	Methods Used	Research findings	Researcher & Year
Superpixel-Oriented Label Distribution Learning for Skin Lesion Segmentation	The superpixels formed by the simple linear iterative cluster (SLIC) algorithm.	Datasets achieve a Dice coefficient reaching 84%, sensitivity 79.6%, precision 80.4%, improved by 19.3%, 8.6%, and 2.5%, respectively, in comparison with the results of U-Net.	Zhou et al. 2022 [13]
A hierarchical three-step superpixel and deep learning framework for skin lesion classification.	A deep learning model (ResNet-50) with three datasets (Ph2, ISBI2016, and HAM1000).	On the datasets, our method achieved an accuracy of 95.40%, 91.1%, and 85.50%,	F. Afza, et.al. 2022[31]
Advancing patient care with AI: a unified framework for medical image segmentation using transfer learning and hybrid feature extraction.	Trained U-Net models to segment skin cancer, polyps, and brain tumor regions from three separate MI datasets (HAM10000, Kvasir-SEG, and Figshare Brain Tumor dataset).	U-Net segmentation achieved high accuracy across datasets, with particularly notable results for polyps (98.00%) and brain tumors (99.66%). LBP features were extracted and classified using an SVM model, achieving 99.22% classification accuracy on the combined dataset (skin, polyp, and brain).	Nazife Çevik., N. 2025 [9]
Foundation-Model-Driven Skin Lesion Segmentation and Classification using SAM-Adapters and Vision Transformers	Integrated foundation-model-based framework that utilizes SAM-Adapter-fine-tuning for lesion segmentation and a ViT-based classifier that incorporates lesion-specific cropping derived from segmentation and cross-attention fusion.	From extensive experimentation, the proposed method outperforms the state-of-the-art segmentation and classification across the dataset. On the ISIC 2018 dataset, it achieves a Dice score of 94.27% for segmentation and an accuracy of 95.88% for classification performance. On PH2, a Dice score of 95.62% is achieved, and for HAM10000, an accuracy of 96.37% is achieved.	Binzagr., f. & Hariri., M. 2026 [29]

III. METHODS

A. SLIC

Enhanced Simple Linear Iterative Clustering (ESLIC) is a superpixel-based segmentation algorithm developed from the Simple Linear Iterative Clustering (SLIC) method. This development was undertaken to improve the ability to segment skin lesions in dermoscopy images, which typically exhibit irregular object boundaries, heterogeneous textures, and complex color variations. Although SLIC is known as an efficient superpixel method with low computational complexity, its performance remains limited when used to separate lesion areas from normal skin tissue, which exhibits very subtle visual differences. Therefore, ESLIC was designed to integrate color, spatial, texture, and gradient information into the superpixel formation process, thereby enabling more adaptive and precise segmentation.

In the initial stage, dermoscopy images that have undergone preprocessing are represented in the CIELAB color space. This color space was chosen because CIELAB is better suited to representing human visual perception than the RGB color space. Each pixel is represented as a feature vector consisting of a luminance component (L_i), a red-green color channel (a_i), a blue-yellow color channel (b_i), and spatial coordinates (x_i, y_i). This representation allows the algorithm to consider both color and pixel position information simultaneously during the segmentation process. Mathematically, the pixel representation [17] is expressed as Eq. (1):

$$P_i = [L_i, a_i, b_i, x_i, y_i] \quad (1)$$

Based on this representation, the color distance between a pixel and the cluster center is calculated using Eq. (2):

$$d_c = \sqrt{(L_i - L_k)^2 + (a_i - a_k)^2 + (b_i - b_k)^2} \quad (2)$$

This equation is used to measure the degree of color similarity between a pixel and the center of a superpixel. The smaller the color distance value obtained, the higher the degree of similarity in color characteristics between the two pixels.

In addition to color information, ESLIC also utilizes spatial information that describes the proximity of pixel positions within an image. Spatial distance is calculated based on the pixel's position coordinates relative to the cluster center using Eq. (3):

$$d_s = \sqrt{(x_i - x_k)^2 + (y_i - y_k)^2} \quad (3)$$

The use of spatial information aims to maintain the continuity of superpixel areas so that pixels that are geographically adjacent in the image are more likely to belong to the same cluster.

Unlike conventional SLIC, which uses a fixed compactness parameter, ESLIC introduces an adaptive compactness mechanism that allows the compactness value to vary according to the local texture characteristics of the image. This approach aims to enable the segmentation process to adapt to the varying lesion structures in different areas of the image. The adaptive compactness value is calculated using the Eq. (4):

$$m_i = m_0(1 + \alpha T_i) \quad (4)$$

In this equation, m_0 is the initial compactness value, is the adaptation factor, and T_i represents the local texture level at the i-th pixel. With this mechanism, areas with more complex textures will receive different compactness values compared to relatively homogeneous areas, making the segmentation more flexible in following the shape of the lesion.

To enhance the segmentation process, ESLIC integrates texture features extracted using the Local Binary Pattern (LBP) method. This method was chosen because it effectively

represents local texture patterns and has been widely used in various medical image processing applications. Once the LBP values are obtained, the texture distance between a pixel and the cluster center is calculated using Eq. (5):

$$d_t = | LBP_i - LBP_k | \quad (5)$$

The integration of texture features allows the algorithm to distinguish between lesion areas and normal skin tissue that share similar color characteristics but have different textures.

In addition to texture, ESLIC also utilizes gradient information to improve segmentation performance in preserving lesion boundaries. Gradient information is obtained using the Sobel operator, which calculates changes in intensity in the horizontal and vertical directions. The total gradient value is calculated using Eq. (6):

$$G = \sqrt{G_x^2 + G_y^2} \quad (6)$$

Next, the gradient distance between a pixel and the cluster center is calculated using Eq. (7):

$$d_g = | G_i - G_k | \quad (7)$$

By utilizing gradient features, ESLIC can identify areas of intensity transition that typically occur at lesion boundaries, allowing the resulting superpixels to follow the object's contours more accurately.

The main contribution of this research lies in the development of a new distance function that combines all color, spatial, texture, and gradient information into a single unified formulation. The ESLIC distance function is formulated as shown in Eq. (8):

$$D_{ESLIC} = \sqrt{d_c^2 + \left(\frac{m_i}{S}\right)^2 d_s^2 + \lambda d_t^2 + \gamma d_g^2} \quad (8)$$

In this equation, d_c represents color distance, d_s represents spatial distance, d_t represents texture distance, and d_g represents gradient distance. The parameter m_i represents adaptive compactness, while S is the interval between superpixel centers. The parameters λ and γ are used as weights that control the contribution of texture and gradient features to the clustering process.

The values of parameters λ and γ, in Eq. (8), were determined empirically through preliminary experiments on a small subset of N images randomly selected from a total of 277 dermoscopy images. The determination was carried out by testing candidate values of λ and γ within a specific range, while the parameters m_0 and α were kept at fixed values for the tested combinations; segmentation quality was evaluated using the Dice Similarity Coefficient (DSC) metric against the ground truth. The values of λ and γ were selected as the final values because they produced the best balance between the contributions of texture and gradient features—that is, a stable DSC value without excessive dominance of any single feature, which, if it occurred, would cause oversegmentation (γ too large) or failure to detect heterogeneous textures in lesions (λ too small).

After the superpixel generation process is complete, ESLIC performs a boundary refinement step to improve the quality of the segmentation boundaries. This step aims to remove any remaining minor noise and smooth the lesion contours so they more closely resemble the actual shape. The refinement process is performed using a combination of morphological operations, namely erosion and dilation. With this stage, lesion boundaries can be better preserved, and segmentation errors at the edges can be minimized.

Based on the proposed formulation and mechanism, ESLIC integrates adaptive compactness adjustment, texture-aware clustering, gradient-aware feature integration, and boundary refinement into a superpixel-based segmentation framework. The combination of these four components enables the formation of superpixels that are more representative of the morphological characteristics of skin lesions, thereby improving segmentation quality and supporting more accurate melanoma classification.

B. Comparison of ESLIC and SLIC

Simple Linear Iterative Clustering (SLIC) is a superpixel-based segmentation method widely used in image processing because it has low computational complexity and is capable of producing relatively uniform superpixels, as shown in Fig. 2. This method works by grouping pixels based on color similarity and spatial proximity, thereby simplifying the image representation without losing important information. However, the application of SLIC [18] to dermoscopy images still faces several limitations. The characteristics of skin lesions—which exhibit high color variation, uneven pigment distribution, heterogeneous texture, and irregular lesion boundaries—mean that conventional SLIC is not yet capable of producing optimal segmentation. Furthermore, the use of a fixed compactness parameter across the entire image area limits the algorithm's ability to adapt to changes in local characteristics.

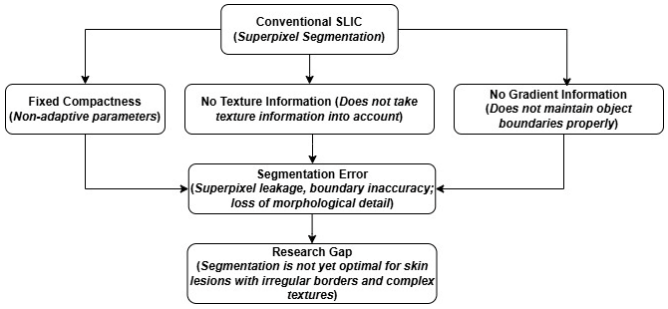

Fig. 2. Conventional SLIC framework

Furthermore, this study provides a comprehensive discussion of the behavior of the ESLIC algorithm. Some of the aspects of the method analyzed are: In the study [1], the convergence criteria used, namely that the iteration is stopped when the average shift in cluster center positions between iterations falls below the threshold ε or the number of iterations reaches the maximum limit of N and in [2], the average number of iterations required to achieve convergence across the entire dataset is 277 images. In [3], a computational stability analysis shows that the number of iterations is relatively consistent for images with homogeneous textures but tends to be higher for lesions with heterogeneous textures and low contrast.

Another limitation of SLIC is its reliance on color and spatial information as the sole basis for the clustering process. In dermoscopy images, lesion areas and normal skin tissue often

share similar colors but differ in texture. When texture information is not taken into account, pixels with similar colors tend to be grouped into the same superpixel even though they originate from different tissue structures. Furthermore, the absence of gradient information makes the algorithm less capable of accurately preserving lesion boundaries, especially in low-contrast areas. This can lead to "*superpixel leakage*"—where portions of normal skin are incorrectly included in the lesion area or vice versa—thereby affecting segmentation quality and reducing the performance of the classification system in subsequent stages. Moreover, to address these limitations, this study proposes Enhanced Simple Linear Iterative Clustering (ESLIC) as an extension of the conventional SLIC method. ESLIC is designed to integrate several new mechanisms: adaptive compactness adjustment, texture-aware clustering, gradient-aware feature integration, and boundary refinement. The adaptive compactness adjustment mechanism allows the compactness parameter to change dynamically based on the local texture characteristics of the image, making the segmentation process more adaptive to the complexity of the lesion. Furthermore, texture information is utilized to improve the algorithm's ability to distinguish between lesion areas and normal skin tissue, while gradient information is used to maintain object boundaries with greater precision. The boundary refinement stage is applied to smooth the segmentation results and reduce errors in the lesion edge areas. By integrating these various mechanisms, ESLIC is expected to produce segmentation results that are more accurate, stable, and representative of the morphological characteristics of skin lesions compared to the conventional SLIC method. The ESLIC framework is shown in detail in Fig. 3.

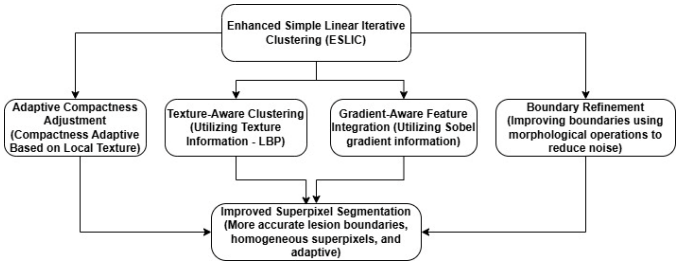

Fig. 3. ESLIC framework

Moreover, to illustrate the limitations of the SLIC method, the distance function used in the superpixel formation process can be expressed as $D = \sqrt{d_c^2 + \left(\frac{m}{s}\right)^2 d_s^2}$, where d_c represents color distance, d_s indicates spatial distance, m is a measure of compactness, and S is the distance between the centers of superpixels. The equation shows that SLIC considers only two main components, namely color and spatial proximity information, in the pixel clustering process. Although this approach is capable of producing computationally efficient segmentation, the lack of texture and gradient information makes the algorithm less capable of representing the complexity of dermoscopy images, which typically exhibit heterogeneous texture patterns, uneven pigment distribution, and irregular morphological lesion boundaries. As a result, the superpixels that are formed often do not optimally follow the contours of the lesion and may lead to segmentation errors, especially at object boundaries with low contrast or complex visual characteristics.

TABLE II. SUMMARY OF HYPERPARAMETERS FOR THE ESLIC IMPLEMENTATION.

Phase / Component	Parameter
Preprocessing	
Contrast stretching	Clipping percentile range (e.g., lower–upper percentile)
Sharpening	Type of kernel / sharpening weight (e.g., unsharp masking)
Top-hat filtering	Size and shape of structuring elements
Normalization	Target intensity range
Feature Extraction	
Local Binary Pattern (LBP)	Radius
Local Binary Pattern (LBP)	Number of neighboring points (P)
Sobel operator	Kernel size
Boundary Refinement	
Morphological operation	Size of structural elements (erosion and dilation)
ESLIC Distance Function	
Start of Compactness	m0
Adaptation factors	α (alpha)
Texture feature weights	λ (lambda)
Gradient feature weights	γ (gamma)
Interval superpixel center	S
Iterative Convergence	
Convergence criteria	Cluster center shift threshold / maximum iterations
Average number of iterations	Mean ± SD across the entire dataset (277 images)

Moreover, to achieve the established research objectives, a structured workflow is required so that each stage of image processing and classification can be carried out systematically. Hyperparameters for the ESLIC implementation are detailed in Table II. This study proposes the Enhanced Simple Linear Iterative Clustering (ESLIC) method as an extension of the conventional SLIC algorithm to improve the quality of skin lesion segmentation in dermoscopy images. The proposed method integrates color, texture, gradient, and spatial information through mechanisms of adaptive compactness adjustment, feature integration, iterative clustering, and boundary refinement. The resulting segmentation is then used as input for a Convolutional Neural Network (CNN) model for skin lesion classification [19], [20]. Overall, the research stages can be seen in Fig. 4. Fig. 4 illustrates that this study begins with dermoscopy images that first undergo preprocessing steps, including grayscale conversion, top-hat filtering, contrast stretching, normalization, and sharpening [21], [22]. Next, the images were processed using the ESLIC algorithm, which consists of superpixel initialization, adaptive compactness, integration of texture and gradient features, iterative clustering, and boundary refinement to produce more accurate lesion segmentation. The segmentation results are then used as input for a CNN to classify melanoma. The system's performance is evaluated using accuracy, precision, recall, and F1-score to arrive at a final decision regarding the type of skin lesion [23]. The algorithms (Pseudocode 1) used in this stage are as follows:

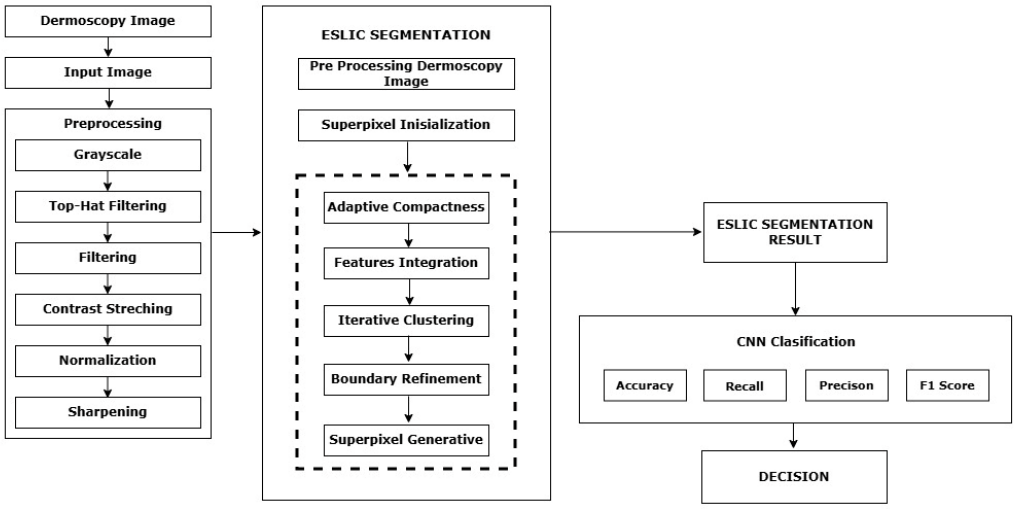

Fig. 4. Research framework

Pseudocode 1:

1. **Input:**
2. Dermoscopic image
3. **Output:**
4. Segmented lesion image S
5. Preprocess the image I
6. Transform the image into the Lab color space
7. Initialize K superpixel centers
8. Extract texture descriptor
9. T = LBP(I)
10. Extract gradient descriptor
11. G = Sobel(I)
12. Compute adaptive compactness
13. mi = m0(1+αTi)
14. For each pixel p do
15. Compute color distance dc
16. Compute spatial distance ds
17. Compute texture distance dt
18. Compute gradient distance dg
19. Compute
20. DESLIC = $\sqrt{(dc^2 + (mi/S)^2 ds^2 + \lambda dt^2 + \gamma dg^2)}$
21. Assign p to the nearest cluster
22. End For
23. Update cluster centers
24. Repeat until convergence
25. Refine the lesion boundary using morphological operations
26. Generate final superpixel
27. Return segmented lesion S

---------- *Pseudocode_1*----------

IV. RESULTS

The first step in this study was to preprocess the dermoscopy images before the segmentation process. The main objective of this step was to improve image quality so that lesion characteristics could be better represented during the segmentation stage. The preprocessing steps used included grayscale conversion, top-hat filtering, contrast stretching, normalization, and sharpening [24]. Grayscale conversion is performed to simplify the image representation and reduce computational complexity [25]. Next, top-hat filtering is used to reduce the effects of artifacts such as hair and lighting variations that frequently appear in dermoscopy images [26]. Following that, contrast stretching is applied to enhance the intensity difference between the lesion area and normal skin tissue [27]. The normalization stage [28], [29] is applied to standardize the image's intensity range, while the sharpening process aims to clarify lesion edges so that object boundaries are more easily recognized during segmentation.

Fig. 5 shows that each preprocessing step improves the visual quality of the image. After sharpening, the lesion boundaries become clearer, and the contrast between the lesion area and the surrounding tissue increases significantly. Once the preprocessing steps are complete, the image is processed using the Enhanced Simple Linear Iterative Clustering (ESLIC) algorithm. This algorithm was developed from the SLIC method by adding mechanisms for adaptive compactness, texture-aware clustering, gradient-aware feature integration, and boundary refinement. The first stage in ESLIC is superpixel initialization. In this stage, the number of superpixels and the initial positions of the cluster centers are determined. Next, an adaptive compactness adjustment is performed to adjust the compactness parameter based on the local texture characteristics of the image. This approach allows for more flexible superpixel formation compared to conventional SLIC. In the next stage, color, texture, gradient, and spatial information features are integrated into the ESLIC distance function. The combination of these features enables the clustering process to distinguish between lesion areas and normal skin tissue more accurately. After the iterative clustering process is complete, a boundary refinement stage is applied to improve the segmentation boundaries and reduce errors in the lesion edge areas.

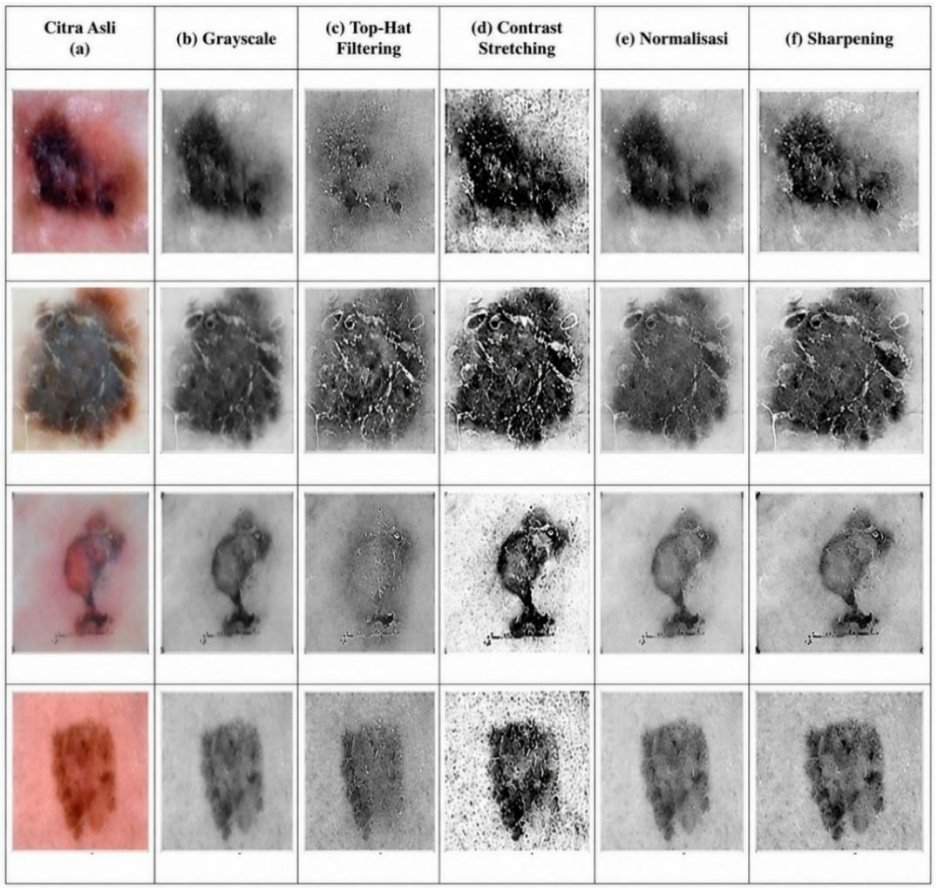

Fig. 5. Pre-processing stage results

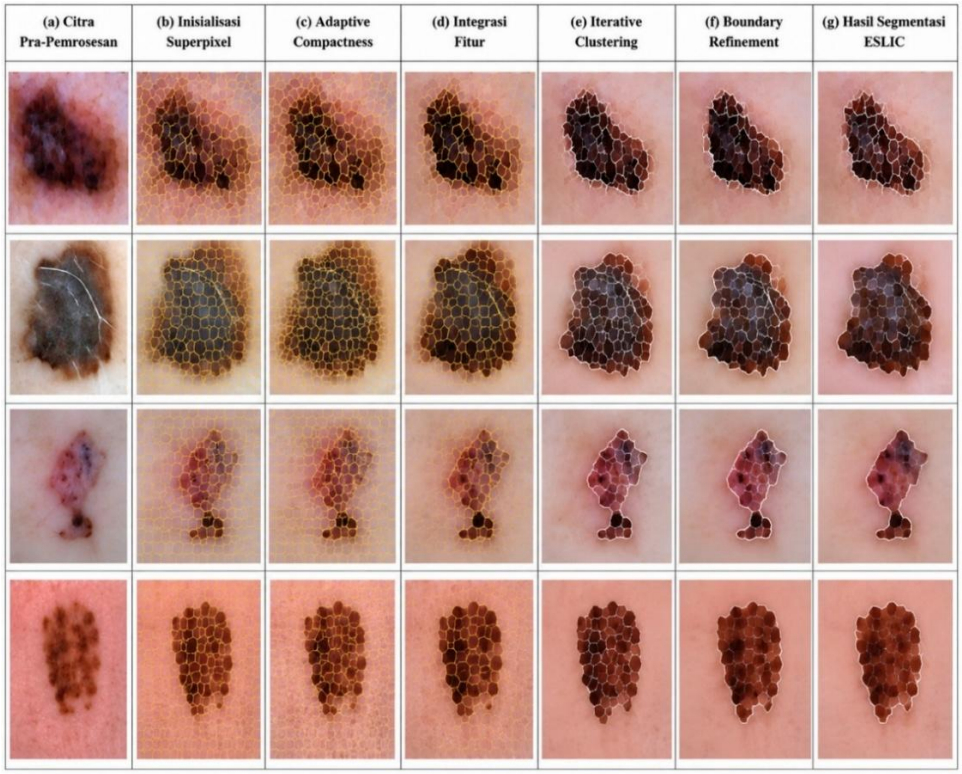

Fig. 6. Segmentation stages using ESLIC.

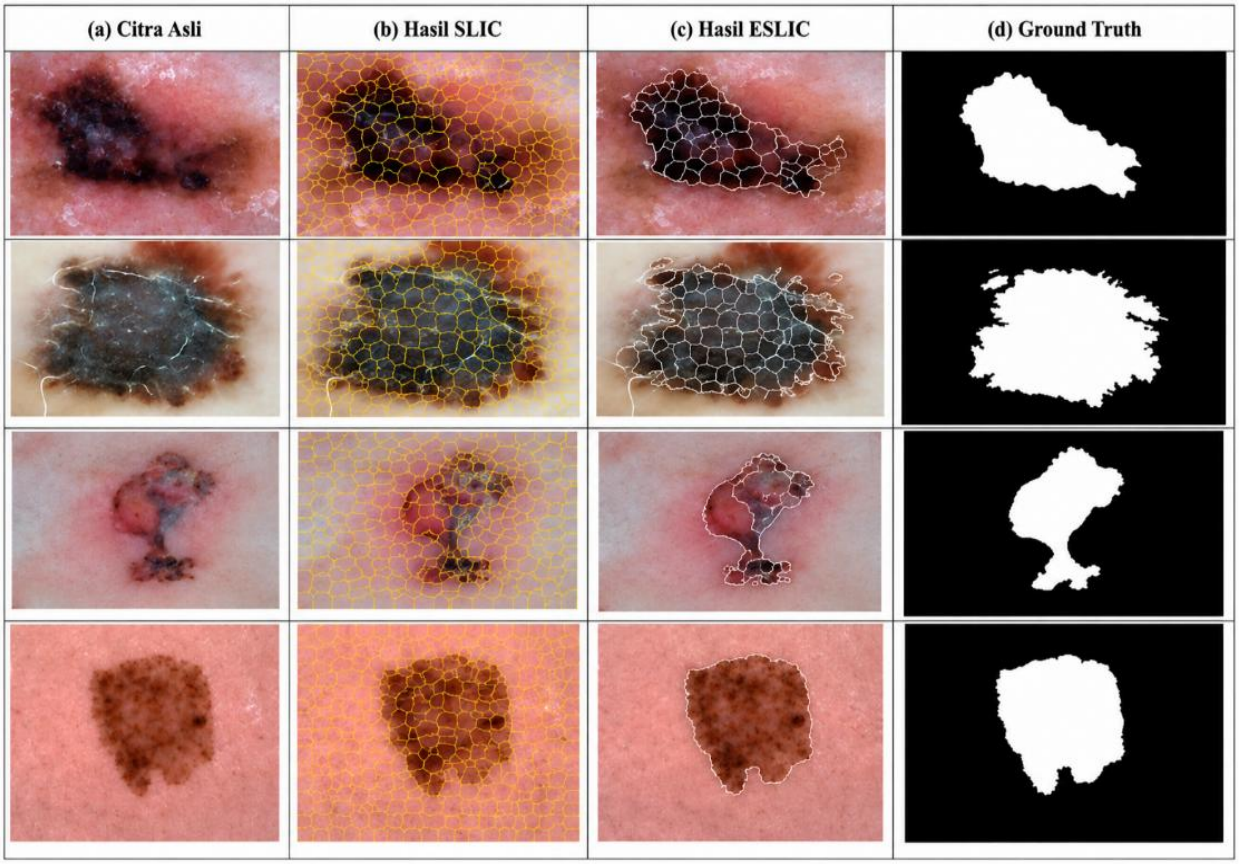

Fig. 7. Comparison of the segmentation results.

Fig. 6 shows that the superpixels generated by ESLIC are able to better follow the morphological structure of the lesion. The boundary refinement stage produces smoother lesion boundaries and reduces superpixel leakage at the object edges. To evaluate the effectiveness of the proposed method, a visual comparison was conducted between conventional SLIC and ESLIC. Comparison of segmentation results is shown in Fig. 7. The segmentation results using SLIC show that some superpixels still straddle lesion boundaries, particularly in areas with complex textures and low contrast. In contrast, ESLIC is able to better preserve lesion contours because it takes texture and gradient information into account during the clustering process. The segmentation results produced by ESLIC appear to be closer to the ground truth than those from the SLIC method. Quantitative evaluation was performed using the Dice Similarity Coefficient (DSC), Jaccard Index (IoU), Boundary F1-Score, and Undersegmentation Error. The detailed segmentation evaluation results are shown in Table III.

TABLE III. SEGMENTATION EVALUATION RESULTS

Method	Dice (%)	IoU (%)	Boundary F1 (%)	Undersegmentation Error
SLIC	87.54	79.33	84.72	0.18
ESLIC	94.26	89.11	92.85	0.07

Table III shows that ESLIC yields improved performance across all evaluation metrics. The Dice score increased by 6.72%, while the IoU increased by 9.78% compared to the SLIC method. Furthermore, the reduction in the Undersegmentation Error indicates that ESLIC is more effective at preserving lesion boundaries during the segmentation process. Quantitative evaluation was performed using the Dice Similarity Coefficient (DSC), Jaccard Index (IoU), Boundary F1-Score, and Undersegmentation Error.

Fig. 8 shows a comparison of the Dice Similarity Coefficient (DSC) and Intersection over Union (IoU) values obtained using the SLIC and ESLIC methods. It can be seen that the ESLIC method yields a Dice value of 94.26% and an IoU of 89.11%, which are higher than those of the SLIC method, which yields a Dice value of 87.54% and an IoU of 79.33%. This improvement indicates that ESLIC is capable of producing more accurate segmentation and has a higher level of agreement with the ground truth. The integration of adaptive compactness, texture-aware clustering, gradient-aware feature integration, and boundary refinement has proven effective in improving the quality of skin lesion segmentation in dermoscopy images. To determine the contribution of each proposed component, a stepwise test was conducted by adding each ESLIC component sequentially.

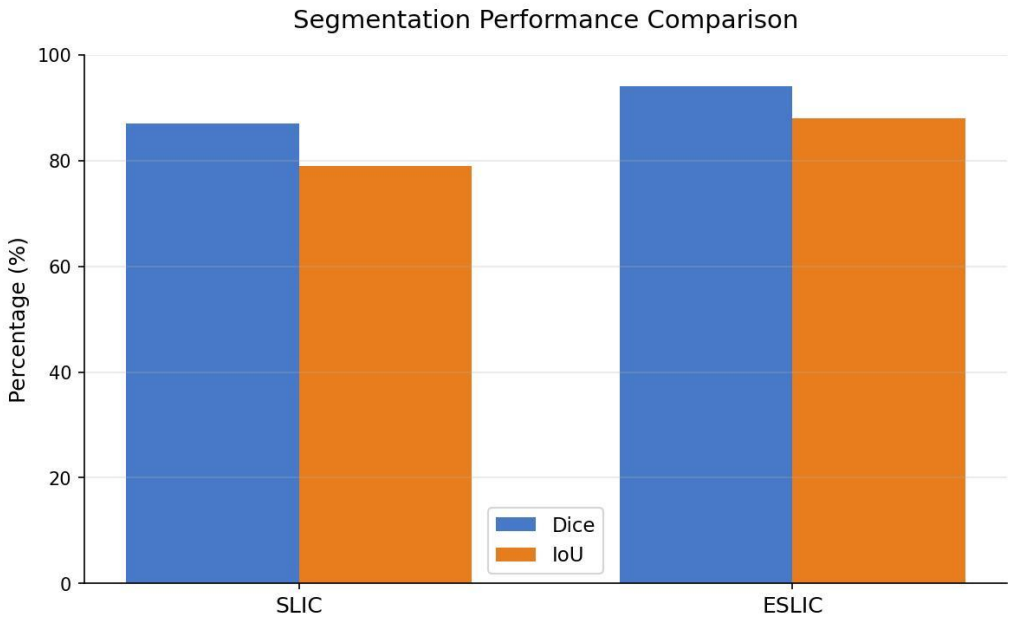

Fig. 8. Comparison of segmentation performance between SLIC and ESLIC.

TABLE IV. ABLATION STUDY OF ESLIC

Method	Dice (%)
SLIC	87.54
SLIC + Adaptive Compactness	89.21
SLIC + Adaptive Compactness + Texture	91.63
SLIC + Adaptive Compactness + Texture + Gradient	93.08
Full ESLIC	94.26

Table IV shows a step-by-step breakdown of the contributions of each ESLIC component, starting with the base SLIC, followed by the addition of adaptive compactness, texture-aware clustering (LBP), gradient-aware feature integration (Sobel), and finally boundary refinement. This approach allows us to demonstrate an increase in the Dice score from 87.54% for SLIC to 94.26% for Full ESLIC. This is not the result of combining all methods, but rather the result of the incremental contributions of each mechanism implemented, with texture feature integration providing the most significant improvement—from 87.54% to 91.63%—followed by gradient and boundary refinement. The test results show that each component contributes to improved segmentation quality. The integration of texture features yields a fairly significant improvement, while the addition of gradient information and boundary refinement results in better preservation of lesion boundaries. The next step is to test the effect of segmentation quality on the classification process using a CNN [30]. In this step, the segmented lesion areas are used as input for the CNN model to classify lesions as benign or malignant.

Table V shows that segmentation using ESLIC yields improved classification performance compared to SLIC. This indicates that better segmentation quality results in a more informative representation of lesions, allowing the CNN to extract discriminative features more effectively.

TABLE V. CNN CLASSIFICATION RESULTS

Method	Accuracy (%)	Precision (%)	Recall (%)	F1-Score (%)
CNN + SLIC	90.12	89.76	89.04	89.40
CNN + ESLIC	96.03	95.88	95.31	95.59

The experimental results show that the integration of adaptive compactness adjustment, texture-aware clustering, gradient-aware feature integration, and boundary refinement successfully improves the quality of skin lesion segmentation in dermoscopy images. Adaptive compactness allows for the formation of superpixels that are more adaptive to local texture variations, while the integration of texture and gradient features enhances the algorithm's ability to preserve complex lesion boundaries. Furthermore, the boundary refinement stage was shown to reduce segmentation errors in object edge regions. This improvement in segmentation quality directly impacts the CNN's classification performance, as evidenced by increases in accuracy, precision, recall, and F1-score. Thus, ESLIC can be considered an effective extension of the SLIC method for AI-based skin lesion segmentation and early melanoma detection applications.

Furthermore, significance tests or statistical analysis are required to determine the percentage (%) of the Descriptive Statistics (Dice) similarity coefficient, as shown in Fig. 9 and Fig. 10. From Fig. 9 and Fig. 10, we find that Descriptive Statistics (Dice %) for SLIC: mean = 87.16, standard deviation = 3.90; for ESLIC: mean = 94.05, standard deviation = 1.80. Lilliefors normality test on paired differences: $p = 0.0093$, shows the distribution of differences is NOT normal; use the Wilcoxon signed-rank test. And based on the data Paired t-test, the value was obtained $t(29) = 8.691$, $p = 0.0000$, 95% CI of mean difference = [5.27, 8.51], as well as the results of Wilcoxon signed-rank test $p = 0.0000$, obtained Cohen's d (paired) = 1.587,

with an interpretation, the improvement in performance with ESLIC compared to SLIC is statistically significant ($p < 0.05$) based on both tests.

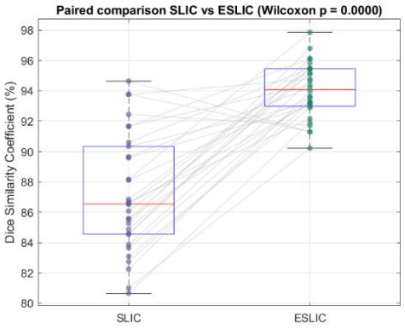

Fig. 9. Paired comparison SLIC vs. ESLIC.

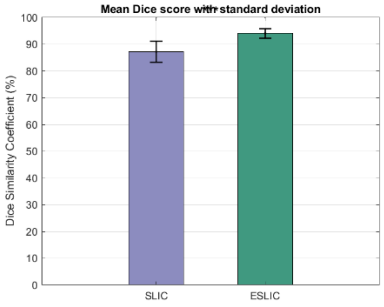

Fig. 10. Mean Dice score with standard deviation.

V. Conclusion

The ESLIC algorithm can be further developed by integrating deep learning-based features, attention mechanisms, or modern segmentation models such as U-Net and Mask R-CNN. In addition, testing on large-scale dermoscopy datasets such as the ISIC Archive is also necessary to evaluate the generalization ability of the proposed method across various skin lesion characteristics.

- This study successfully developed the Enhanced Simple Linear Iterative Clustering (ESLIC) method as an extension of the conventional SLIC algorithm for skin lesion segmentation in dermoscopy images. This development was achieved through the integration of adaptive compactness adjustment, texture-aware clustering, gradient-aware feature integration, and boundary refinement to improve segmentation performance in lesion areas with complex characteristics.
- The integration of color, texture, gradient, and spatial information into the ESLIC distance function enables the generation of superpixels that are more adaptive to variations in skin lesion morphology. This approach has been shown to improve the algorithm's ability to preserve lesion boundaries and reduce the phenomenon of superpixel leakage, which is still commonly found in conventional SLIC methods.
- Segmentation evaluation results show that ESLIC performs better than SLIC. The proposed method achieved a Dice Similarity Coefficient (DSC) of 94.26% and an Intersection over Union (IoU) of 89.11%, indicating a high level of agreement with the ground truth of skin lesion segmentation.
- Testing the contribution of algorithm components shows that each mechanism added to ESLIC improves segmentation performance. The combination of adaptive compactness, texture features, gradient features, and boundary refinement collectively produces more stable and accurate segmentation quality compared to the standard SLIC method.
- Better segmentation quality has a positive impact on the Convolutional Neural Network (CNN)-based melanoma classification process. Using ESLIC segmentation results as CNN input improves classification accuracy to 96.03%, demonstrating that ESLIC has high potential for application in AI-based early melanoma detection systems to support more accurate and efficient diagnosis.

VI. Future Research

A dataset of 277 dermoscopy images is relatively small for drawing broad conclusions about the algorithm's generalizability. We obtained this data from Dr. M. Djamil General Hospital in Padang, which includes cases of benign lesions and melanoma; however, further validation on a larger and more diverse dataset is needed to confirm the robustness and generalization of ESLIC. Testing on large-scale public datasets such as the ISIC Archive is an important step toward a comprehensive evaluation. There are still limitations to this research: the comparison in this study is limited to conventional superpixel methods (SLIC) and does not yet include deep learning-based segmentation architectures such as U-Net or Mask R-CNN, which have demonstrated higher Dice/IoU scores on dermoscopy datasets. In our discussion, we position ESLIC not as a direct competitor to deep learning methods, but rather as a computationally lighter approach that does not require large amounts of pixel-annotated mask data for training. The strength of this research is that it includes 277 images, and the next step is to directly compare it with U-Net and Mask R-CNN on the same dataset.

Future analysis needs to be significantly improved; ESLIC needs to produce segmentation that is even more accurate than the ground truth, and issues such as low contrast between lesions and skin, as well as the preprocessing stage and lesion boundaries, still need to be addressed to improve image quality, such as low contrast, light reflection, and diffuse lesion borders. Future research will also conduct a detailed comparative analysis of the average Dice scores and IoU by category to highlight significant differences between SLIC and ESLIC, as well as other more detailed parameters.

References

[1] S. Kumar, "Early Disease Detection Using AI: A Deep Learning Approach to Predicting Cancer and Neurological Disorders," Int. J. Sci. Res. Manag., vol. 13, no. 04, pp. 2136–2155, Apr. 2025, doi: 10.18535/ijsrm/v13i04.mp02.

[2] S. Fatima, M. U. Akram, S. Mohammad, and S. Bin Ahmed, "Deep learning in dermatopathology: applications for skin disease diagnosis and classification," Sep. 01, 2025, Springer Nature. doi: 10.1007/s42452-025-07138-3.

[3] P. Weber, P. Tschandl, C. Sinz, and H. Kittler, "Dermatoscopy of Neoplastic Skin Lesions: Recent Advances, Updates, and Revisions," Nov. 01, 2018, Springer New York LLC. doi: 10.1007/s11864-018-0573-6.

[4] H. Eghtesaddoust, M. Valizadeh, and M. C. Amirani, "Fusion of Deep and Time–Frequency Local Features for Melanoma Skin Cancer Detection," Appl. Comput. Intell. Soft Comput., vol. 2025, no. 1, 2025, doi: 10.1155/acis/4767052.

[5] P. Ordóñez, Y. Xie, X. Zhang, C. Y. Xie, S. Acosta, and I. Gutiérrez, "SPADE: Superpixel Adjacency Driven Embedding for Three-Class Melanoma Segmentation," Algorithms, vol. 18, no. 9, Sep. 2025, doi: 10.3390/a18090551.

[6] M. A. Kassem, K. M. Hosny, R. Damaševičius, and M. M. Eltoukhy, "Machine learning and deep learning methods for skin lesion classification and diagnosis: A systematic review," Aug. 01, 2021, Multidisciplinary Digital Publishing Institute (MDPI). doi: 10.3390/diagnostics11081390.

[7] F. Hu et al., "Advances in intelligent recognition and diagnosis of skin scar images: concepts, methods, challenges, and future trends," 2025, Frontiers Media SA. doi: 10.3389/fmed.2025.1667087.

[8] A. R. Ali, J. Li, and S. J. O'Shea, "Towards the automatic detection of skin lesion shape asymmetry, color variegation and diameter in dermoscopic images," PLOS ONE, vol. 15, no. 6, Jun. 2020, doi: 10.1371/journal.pone.0234352.

[9] N. Çevik, T. Çevik, O. Osman, S. Alsubai, and J. Rasheed, "Advancing patient care with AI: a unified framework for medical image segmentation using transfer learning and hybrid feature extraction," Front. Med., vol. 12, 2025, doi: 10.3389/fmed.2025.1589587.

[10] J. A. Fee, F. P. McGrady, and N. D. Hart, "Dermoscopy use in primary care: a qualitative study with general practitioners," BMC Prim. Care, vol. 23, no. 1, Dec. 2022, doi: 10.1186/s12875-022-01653-7.

[11] R. Achanta, A. Shaji, K. Smith, A. Lucchi, P. Fua, and S. Süsstrunk, "SLIC superpixels compared to state-of-the-art superpixel methods," IEEE Trans. Pattern Anal. Mach. Intell., vol. 34, no. 11, pp. 2274–2281, 2012, doi: 10.1109/TPAMI.2012.120.

[12] S. Adamu et al., "The future of skin cancer diagnosis: a comprehensive systematic literature review of machine learning and deep learning models," 2024, Cogent OA. doi: 10.1080/23311916.2024.2395425.

[13] Q. Zhou, T. He, and Y. Zou, "Superpixel-Oriented Label Distribution Learning for Skin Lesion Segmentation," Diagnostics, vol. 12, no. 4, Apr. 2022, doi: 10.3390/diagnostics12040938.

[14] D. Xu, T. Katzke, and E. Müller, "From Pixels to Graphs: Deep Graph-Level Anomaly Detection on Dermoscopic Images," Aug. 2025, [Online]. Available: http://arxiv.org/abs/2508.11826

[15] A. Jiménez-Sánchez et al., "In the Picture: Medical Imaging Datasets, Artifacts, and their Living Review," in ACMF AccT 2025 - Proceedings of the 2025 ACM Conference on Fairness, Accountability, and Transparency, Association for Computing Machinery, Inc, Jun. 2025, pp. 511–531. doi: 10.1145/3715275.3732035.

[16] A. H. Roky et al., "Overview of skin cancer types and prevalence rates across continents," Mar. 01, 2025, Chinese Medical Association. doi: 10.1016/j.cpt.2024.08.002.

[17] T. Nagaoka, "Improved Skin Lesion Segmentation in Dermoscopic Images Using Object Detection and Semantic Segmentation," Clin. Cosmet. Investig. Dermatology , vol. 18, pp. 1191–1198, 2025, doi: 10.2147/CCID.S518751.

[18] K. Suwais, K. Alheeti, and D. Al_Dosary, "A Review on Classification Methods for Plants Leaves Recognition," Int. J. Adv. Comput. Sci. Appl., vol. 13, no. 2, pp. 92–100, 2022, doi: 10.14569/IJACSA.2022.0130211.

[19] S. R. Waheed et al., "Melanoma Skin Cancer Classification based on CNN Deep Learning Algorithms," Malaysian J. Fundam. Appl. Sci., vol. 19, no. 3, pp. 299–305, 2023, doi: 10.11113/mjfas.v19n3.2900.

[20] H. Naseri and A. A. Safaei, "Diagnosis and prognosis of melanoma from dermoscopy images using machine learning and deep learning: a systematic literature review," Dec. 01, 2025, BioMed Central Ltd. doi: 10.1186/s12885-024-13423-y.

[21] H. T. Halawani, E. M. Senan, Y. Asiri, I. Abunadi, A. M. Mashraqi, and E. A. Alshari, "Enhanced early skin cancer detection through fusion of vision transformer and CNN features using hybrid attention of EViT-Dens169," Sci. Rep., vol. 15, no. 1, Dec. 2025, doi: 10.1038/s41598-025-18570-1.

[22] L. N. Zulita, S. Defit, and Sumijan, "Detecting Skin Threats: A Superpixel-Based Analysis of Melanoma," in ICAISD 2025 - 2025 International Conference on Advanced Information Scientific Development: Artificial Intelligence: Advancing Research and Computational Innovations for Global Welfare, Proceedings, Institute of Electrical and Electronics Engineers Inc., 2025, pp. 78–83. doi: 10.1109/ICAISD68166.2025.11385687.

[23] A. A. Abdulredah, M. A. Fadhel, L. Alzubaidi, Y. Duan, M. Kherallah, and F. Charfi, "Towards unbiased skin cancer classification using deep feature fusion," BMC Med. Inform. Decis. Mak., vol. 25, no. 1, Dec. 2025, doi: 10.1186/s12911-025-02889-w.

[24] S. A. Alzakari et al., "LesionNet: an automated approach for skin lesion classification using SIFT features with customized convolutional neural network," Front. Med., vol. 11, 2024, doi: 10.3389/fmed.2024.1487270.

[25] N. Sarwar, A. Irshad, Q. H. Naith, K. D.Alsufiani, and F. A. Almalki, "Skin lesion segmentation using deep learning algorithm with ant colony optimization," BMC Med. Inform. Decis. Mak., vol. 24, no. 1, Dec. 2024, doi: 10.1186/s12911-024-02686-x.

[26] S. M. Thwin and H. S. Park, "Enhanced Skin Lesion Segmentation and Classification Through Ensemble Models," Eng, vol. 5, no. 4, pp. 2805–2820, Dec. 2024, doi: 10.3390/eng5040146.

[27] H. A. Owida et al., "A deep learning-based dual-branch framework for automated skin lesion segmentation and classification via dermoscopic Images," Sci. Rep., vol. 15, no. 1, Dec. 2025, doi: 10.1038/s41598-025-21783-z.

[28] A. S. Al-Waisy, S. Al-Fahdawi, M. I. Khalaf, M. A. Mohammed, B. Al-Attar, and M. N. Al-Andoli, "A deep learning framework for automated early diagnosis and classification of skin cancer lesions in dermoscopy images," Sci. Rep., vol. 15, no. 1, Dec. 2025, doi: 10.1038/s41598-025-15655-9.

[29] F. Binzagr and M. Hariri, "Foundation-Model-Driven Skin Lesion Segmentation and Classification Using SAM-Adapters and Vision Transformers," Diagnostics, vol. 16, no. 3, Feb. 2026, doi: 10.3390/diagnostics16030468.

[30] D. Moturi, R. K. Surapaneni, and V. S. G. Avanigadda, "Developing an efficient method for melanoma detection using CNN techniques," J. Egypt. Natl. Canc. Inst., vol. 36, no. 1, 2024, doi: 10.1186/s43046-024-00210-w.

[31] F. Afza, M. Sharif, M. Mittal, M. A. Khan, and D. J. Hemanth, "A hierarchical three-step superpixels and deep learning framework for skin lesion classification," Methods, vol. 202, pp. 88–102, Jun. 2022, doi: 10.1016/j.ymeth.2021.02.013.